Effect of iterative reconstruction on image quality in evaluating patients with coronary calcifications or stents during coronary computed tomography angiography: a pilot study

Ezgi Güler, Volkan Vural, Emre Ünal, Ilgaz Çağatay Köse, Deniz Akata, Muşturay Karcaaltıncaba, Tuncay Hazırolan

Department of Radiology, Faculty of Medicine, Hacettepe University; Ankara-*Turkey*

ABSTRACT

Objective: To determine the effect of "Iterative Reconstruction in Image Space" (IRIS) on image quality by comparing reconstructions of both medium and sharp kernels when evaluating coronary calcifications or stents during coronary computed tomography (CT) angiography.

Methods: Thirty one consecutive patients were scanned with an electrocardiogram-gated helical technique on a dual-source CT system. Image reconstruction was performed using standard filtered back projection (FBP) and IRIS algorithm on both medium and sharp kernels (B26f, I26f, B46f, I46f). Each reconstruction was derived from the same raw data. Two blinded readers graded image quality using a five-point scale. Noise, signal-to-noise ratio (SNR), contrast-to-noise ratio (CNR) were obtained. Noise was derived from the ascending aorta and left ventricle. SNR was obtained from sinus Valsalva, interventricular septum, and coronary vessels. CNR was obtained from septum, coronary vessels, and left ventricle. Comparisons of paired results between FBP and IRIS images were analyzed using the repeated measures analysis of variance method. Interreader correlation was assessed using weighted Kappa statistic.

Results: Noise values of the ascending aorta and left ventricle were significantly lower in the images reconstructed with IRIS than those reconstructed with FBP for the evaluation of the same filters. SNR and CNR values were higher in the IRIS images ($p<0.05$). Interreader agreement for four reconstructions was interpreted as moderate ($\kappa=0.40$–0.59).

Conclusion: IRIS significantly reduced image noise and improved imaging of coronary calcifications or stents. When combined with a sharp kernel, IRIS can improve image quality by reducing the negative effects of decreased signal that may result from using a sharp kernel. *(Anatolian J Cardiol 2016; 16: 119-24)*

Key words: coronary computed tomography angiography, iterative reconstruction, coronary calcification, stent

Introduction

With technological advancements in multidetector computed tomography (CT), coronary CT angiography has become a preferred non-invasive alternative to conventional coronary angiography to evaluate coronary artery stenosis (1-3).

However, the radiation dose associated with coronary CT angiography is high and clinically significant; thus, reduction of dose value is important. Many dose-saving methods were applied in recent CT generations, including prospective electrocardiogram (ECG)-gating protocols, lower tube voltage application, tube current modulation, and high pitch acquisition (4-7).

When using the standard CT reconstruction techniques [filtered back projection (FBP)], lower radiation dose causes an increase in image noise. Recently, iterative reconstruction has been more frequently used in coronary CT angiography to reduce radiation dose and improve image quality (8, 9).

The evaluation of coronary calcifications and stents can be challenging owing to limitations of CT such as high attenuation and "blooming artifacts" (10). To reduce artifacts, sharp kernels are commonly used, but this results in lowering the signal-to-noise ratio (SNR).

The application of iterative reconstruction methods may be useful at overcoming the difficulties in the evaluation of calcifi-

Table 1. Patient and scanning protocol characteristics

Characteristics and parameters	Data (n=31)
Age, years	62.3±11.2
Sex (male/female)	n=18/ n=13
BMI	29.6±5.2
Heart rate	70.3±11.8
Tube potential (kVp)	
120 kVp	n=28
140 kVp	n=3
Tube current (mAs)	246.7±58.8

Data are presented as mean±SD or number.
BMI - body mass index; n - number of patients

Figure 1. a, b. B46f image (a) and I46f image (b) show a coronary stent in the left anterior descending artery in a 52-year-old male patient

cations and stents. In the "Iterative Reconstruction in Image Space" (IRIS) algorithm, a master image is generated from the raw data. This master image contains all relevant information for further corrections and is then used as the reference image. The following iterative corrections known from theoretical iterative reconstruction are consecutively performed in image space based on the master image. After a few iterations in image space, image noise is significantly reduced, whereas other parameters such as image sharpness are maintained. Therefore, the time-consuming repeated projection and corresponding back projection from the raw data can be avoided.

Hence, the purpose of our study was to determine the effect of the IRIS algorithm on image quality by comparing reconstructions of both medium and sharp kernels when evaluating coronary calcific plaques or stents at CT angiography. Although IRIS is a known technique for radiation dose reduction, our study solely focused on its effect on image quality.
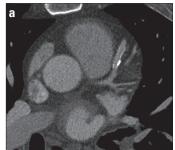
Methods

Patients

This prospective study was approved by our Institutional Review Board. Written informed consent was obtained from each patient. The study population consisted of 31 patients (18 men, 62.3±11.2 years). All patients had coronary calcifications; 9 of the patients had coronary stents. The mean body mass index (BMI) was 29.6±5.2. According to the World Health Organization (WHO) classification, 4 patients were classified as normal weight (BMI 18.5-24.9), 16 were overweight (BMI 25-29.9), 5 were obese class I (BMI 30-34.9), 5 were obese class II (BMI 35-39.9), and 1 was obese class III (BMI≥40). Patient and scanning protocol characteristics are detailed in Table 1.

Patients who had arrhythmia, allergy to contrast media, and with non-calcified plaques were excluded.

Scanning protocol and reconstruction

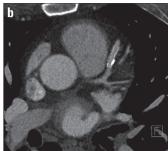Cardiac CT angiography was performed on a first generation dual-source CT system (SOMATOM Definition, Siemens Healthcare, Forchheim, Germany). The CT scan protocol was defined by patient age, BMI, heart rate/rhythm, and scan indication. CT protocols included retrospective ECG-gating and prospective ECG-triggering (prospective ECG triggering was applied to patients with heart rates lower than 65 per min).

Contrast medium enhancement was achieved by injection of 80 mL of iodinated contrast material (iomeprol, iomeron 400 mg I/mL; Bracco, Milan, Italy) injected at 5-6 mL/s followed by a saline flush of 30-40 mL through an 18 or 20 G intravenous antecubital catheter using a dual-syringe injector (CT Contrast Agent Injector, Ulrich Medical Systems, Ulm, Germany). Bolus was tracked using an automated bolus triggering technique in the ascending aorta (CARE Bolus; Siemens Healthcare, Forchheim, Germany). Examination was automatically started 7 s after the triggering threshold [100 Hounsfield Unit (HU)] was reached.
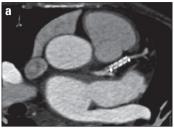
CT images were acquired with a detector collimation of 2 x 32 x 0.6 mm and a gantry rotation time of 0.33 s. A 120 kV tube potential was used in patients with a BMI of >25 kg/m^2, whereas for 3 patients with a BMI of >30 kg/m^2, the tube potential was increased to 140 kV.
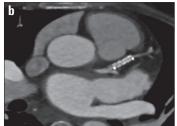
For the retrospective ECG-gating, the ECG tube current modulation technique was used as the tube current (mAs) was changed during the examination for each body part. In 30%-80% of the R-R intervals, maximum effective mAs was set, and during the rest of the R-R interval, mA was lowered to 20% of the effective dose. Step and shoot method was used for the prospective ECG-triggering as the X-ray tube was on only in 70% of the R-R interval.

Best systolic or best diastolic phase images were reconstructed using traditional FBP and a medium (B26f) kernel. The IRIS technique was applied to raw data using a medium kernel (I26f). Moreover, high-resolution sharp reconstruction kernel for FBP reconstructions (B46f) and its corresponding algorithm for IRIS reconstructions (I46f) were acquired (Fig. 1 and Fig. 2). All reconstructed images were obtained with a slice thickness of 0.75 mm in 0.4 mm increments. The best phase was selected for reconstruction and analysis. The same phase was used for both reconstructions.

Image analysis

FBP and iterative reconstructions were transferred to an image processing workstation (Leonardo, Siemens AG, Healthcare Sector, Forchheim, Germany).
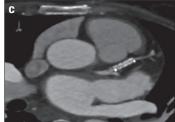
Figure 2. a-d. B26f image (a), I26f image (b), B46f image (c), and I46f image (d) demonstrate a coronary stent in the left anterior descending artery

To obtain objective image quality, image noise, SNR, and contrast-to-noise ratio (CNR) were calculated for images of both the FBP and IRIS algorithms in two kernels. Image noise was derived from the standard deviation of density values. Image noise was measured using a circular region of interest (ROI) (area of 100 mm^2) placed in the contrast-enhanced lumen of the ascending aorta and left ventricle on FBP and corresponding IRIS images on both medium and sharp kernels, respectively. SNR was derived from sinus Valsalva, interventricular septum, left anterior descending coronary artery (LAD), circumflex artery (Cx), and right coronary artery (RCA). SNR was calculated by placing a circular ROI (area of 30 mm^2 placed to interventricular septum and area of 5 mm^2 placed to proximal coronary vessels) to each mentioned location. Mean density was measured, and SNR was obtained with the division by image noise. For four reconstruction series (B26f, I26f, B46f, and I46f), all calculations were made from the same locations. Three CNR values were obtained for each reconstruction. The first location of CNR was defined as the difference between the mean density of the contrast-filled left ventricular chamber and the mean density of the septum, which was then divided by image noise (CNR left ventricle/septum). The two other CNR values were acquired from the septum and LAD (CNR septum/coronary vessel) and from the left ventricle and LAD (CNR left ventricle/coronary vessel).

Subjective image analysis was performed by two independent, blinded readers (two radiologists with 5 years of experience in cardiovascular imaging). One hundred twenty-four data sets (31 B26f, 31 I26f, 31 B46f, 31 I46f) were viewed in a randomized order. Each reader rated each data set using a 5-point Likert scale according to image noise, coronary wall definition, contrast resolution, and general image impression. The Likert scale was defined as follows: 1: poor image quality, poor vessel wall definition, poor assessment of stents; 2: adequate, reduced image quality with poor vessel wall definition or increased image noise, fair assessment of stents; 3: good, good image noise, limitations of low contrast resolution and vessel wall definition are minimal, good assessment of stents; 4: very good, very good attenuation of vessel lumen and delineation of contours, coronary wall definition, very good assessment of stents; 5: excellent, excellent attenuation of the vessel lumen and clear delineation of the vessel walls, limited image noise, excellent assessment of stents.

Statistical analysis

Statistical analysis was performed using a dedicated statistical software (SPSS for Windows, Version 18.0. SPSS Inc., Chicago, IL, USA). Numerical quantitative data variables are expressed as mean value±standard deviation. Comparisons of paired results between the FBP and IRIS images in each protocol were analyzed using the repeated measures analysis of variance method with two repeated factors. Pairwise comparisons were done by the Bonferroni test. A p value of <0.05 was considered statistically significant. The Shapiro-Wilk test was used to assess the distribution of continuous variables. For non-normally distributed variables, the Friedman test was used to compare the differences. When the differences were significant in the Friedman test, Dunn's multiple comparison test was used to determine the group/groups that created the differences. Interreader agreement for image quality was evaluated with κ statistics (weighted Kappa). The correlation was classified as moderate (κ=0.40–0.59); good (κ=0.60-0.79), and excellent (κ>0.80).

Results

Objective comparison of image quality between FBP and IRIS

The noise values of the aorta and left ventricle were significantly lower in data sets obtained by IRIS compared with those using the FBP technique (p<0.05).

SNR (obtained from sinus Valsalva, septum, LAD, Cx, and RCA) and CNR (septum/coronary vessel, left ventricle/coronary vessel, and left ventricle/septum) were significantly higher in IRIS compared with FBP when using the same filters. For the comparisons of reconstructions in terms of SNR and CNR, there was not only a significant difference between the couples of FBP and IRIS on the same filters (B26f-I26f, B46f-I46f, respectively) but also in the couples of different filters (B26f-B46f and I26f-I46f) (p<0.05). Table 2 provides the mean values of objective image quality parameters for each group in detail.

According to the results of the Shapiro-Wilk test, all objective image quality parameters except SNR obtained from septum (B26f, I26f, B46f, I46f) and CNR obtained from left ventricle/coronary vessel (B26f, I26f, B46f, I46f) were normally distributed. Because these two variables were not normally distributed, the Friedman test was used to compare the differences between four reconstructions (B26f, I26f, B46f, I46f). The results showed

Table 2. Objective image quality parameters in each reconstruction protocol

					P			
					B	**I**	**26F**	**46F**
	B26f	**I26f**	**B46f**	**I46f**	**26-46**	**26-46**	**B-I**	**B-I**
Noise (aorta)	23.4±4.3	16.9±2.9	35.6±7.4	28.7±6.6	<0.001	<0.001	<0.001	<0.001
Noise (L ventricle)	26.3±5.2	20.8±4.0	47.9±8.4	37.7±7.8	<0.001	<0.001	<0.001	<0.001
SNR sinus Valsalva	17.1±4.8	23.8±5.7	11.3±3.6	13.9±4.2	<0.001	<0.001	<0.001	<0.001
SNR septum	4.4±1.5	6.3±1.9	3.1±1.2	3.9±1.3	<0.001	<0.001	<0.001	<0.001
SNR LAD	15.3±5.7	21.2±7.7	10.3±3.4	12.6±4.4	<0.001	<0.001	<0.001	<0.001
SNR Cx	15.7±5.4	21.6±7.2	10.5±3.8	13±4.8	<0.001	<0.001	<0.001	<0.001
SNR RCA	16.2±5.5	22.1±6.5	10.6±3.4	13±4.2	<0.001	<0.001	<0.001	<0.001
CNR septum/coronary	10.9±5	15.1±6.4	7.1±2.8	8.7±3.7	<0.001	<0.001	<0.001	<0.001
CNR L ventricle/coronary	2.8±3	4.4±4.3	1.6±1.8	1.9±2.2	0.013	<0.001	<0.001	0.011
CNR L ventricle/septum	11.5±3.6	16.3±4.9	7.7±2.6	9.5±3.6	<0.001	<0.001	<0.001	<0.001

Data are presented as mean±SD.
CNR - contrast-to-noise ratio; Cx - circumflex artery; L ventricle - left ventricle; LAD - left anterior descending artery; SNR - signal-to-noise ratio; RCA - right coronary artery
B26f, B46f - filtered back projection reconstructions derived from medium and sharp kernels, respectively.
I26f, I46f - IRIS reconstructions derived from medium and sharp kernels, respectively. The repeated measures analysis of variance method with two repeated factors and Bonferroni test.

Table 3. Subjective image quality. Mean scores assessed by two radiologists

	Radiologist 1	**Radiologist 2**	**Kappa (κ)**
B26f	3.58±0.50	3.74±0.44	0.510
I26f	4±0.52	4.39±0.61	0.417
B46f	3.71±0.46	3.97±0.60	0.485
I46f	4.45±0.50	4.61±0.49	0.558

Data are presented as mean±SD.
B26f, B46f - filtered back projection reconstructions derived from medium and sharp kernels, respectively.
I26f, I46f - IRIS reconstructions derived from medium and sharp kernels, respectively.
Weighted Kappa

that there was no statistically significant difference between SNR obtained from septum in B26f and I26f reconstructions (p=1.0). However, there was a statistically significant difference between the comparisons of other reconstruction couples for the evaluation of SNR obtained from septum (p<0.05). As for CNR left ventricle/coronary vessel assessment, there was no statistically significant difference between couples of B46f-I46f, B46f-B26f, and I46f-B26f (p>0.05).

Nine patients who had coronary stents were separately evaluated, and differences between FBP and IRIS for this group were calculated using the Friedman test. Noise, SNR, and CNR obtained from previously described locations at four different reconstructions (B26f, I26f, B46f, and I46f) were analyzed. The results demonstrated that there was a statistically significant difference between B26f and I26f and also between B46f and I46f reconstructions for the evaluation of each objective image quality parameter.

Subjective comparison of image quality between FBP and IRIS

The mean values of subjective evaluation scores and κ statistic for image quality are shown in Table 3. The highest mean values of scores were given for I46f images by both readers. Interreader agreement for four reconstructions (B26f, I26f, B46f, and I46f) was interpreted as moderate agreement (κ=0.40–0.59). Although correlation between two radiologists was classified as moderate, the highest value of κ was calculated for the I46f group (κ=0.558).

Discussion

The findings of our study revealed that IRIS could significantly reduce image noise and improve the imaging of coronary calcifications or stents compared with traditional FBP.

Advances in CT technology have increased the reliability and accuracy of coronary CT angiography to exclude coronary artery stenosis when compared with conventional coronary angiography (11, 12). However, there are some limitations of coronary CT angiography that can reduce or alter the diagnosis. For example, the presence of heavy coronary artery calcifications or metallic stents especially in patients with a high BMI can reduce the diagnostic performance of coronary CT angiography (13). Metallic struts of stents or density calcified plaques can produce blooming artifacts that can limit the accurate evaluation of coronary artery lumen (13, 14).

Blooming artifacts are mainly due to beam hardening. The metal struts or dense calcifications can cause beam hardening, where lower energy photons are absorbed. Consequently, the beam is more intense when it reaches the detectors (15). Blooming artifacts can be reduced by high kV imaging, but this could result in an increased dose of radiation and should not be preferred. Other techniques to minimize artifacts are the improvement of spatial resolution and the use of sharp kernels to enhance the edges of the high attenuation structures. However, using sharp kernels may lead to a decrease in the signal.

In the present study, we found that image noise in the aorta and left ventricle in images constructed with sharp kernels were higher than those constructed with medium kernel. However, for the comparison between same kernels, images constructed with IRIS had lower noise both in the aorta and left ventricle. When B26f-I26f and B46f-I46f were compared, there was a statistically significant difference for each pair regarding noise, SNR, and CNR (p<0.05). Similar to our findings, there are several studies in literature illustrating that iterative reconstruction could reduce image noise. Ebersberger et al. (16) reported that iterative reconstruction significantly improves imaging of coronary artery stents compared with FBP in a study that consisted of 37 implanted stents that were reconstructed at full- and half-radiation doses. Oda et al. (14), who combined hybrid iterative reconstruction technique with high-resolution kernels, stated that it reduced the image noise and coronary stent blooming artifacts and led to a better diagnostic performance for the detection of in-stent stenosis. Hou et al. (17) concluded that iterative reconstruction could provide equivalent or improved coronary image quality on coronary CT angiography compared with routine-dose FBP while enabling radiation dose reductions of 55%.

Many studies have shown that iterative reconstruction techniques reduce radiation dose in coronary CT angiography (18-20). However, this was not the subject of our current study. In our investigation, we solely focused on the effect of IRIS and combination of IRIS with high-resolution kernels on the image quality of coronary CT angiography.

In our study, the subjective evaluation of image quality showed that sharp kernel-reconstructed images had higher scores than medium kernel-reconstructed images. It agreed with the study that recommended sharp kernel use for the assessment of stent lumen as it reduces blooming artifacts (15). We found that sharp kernel images reconstructed with IRIS had the highest scores given by both readers. In a recent study, sharp kernel images constructed with IRIS were considered the optimal images to observe coronary stents (21). Our findings also suggested that when combined with a sharp kernel, IRIS eliminated the potential negative effects of decreased signal on image quality that may be caused using a sharp kernel.

Study limitations

Our study has several limitations. First, it included a small number of patients because it was a pilot study in our institution. Second, we did not evaluate diagnostic performance using different stent sizes and types, although these factors affected the visibility of the stent lumen. Third, because of our small number of patients, division into subgroups according to BMI was limited. Therefore, the effect of IRIS on the image quality of patients with higher BMI could be more accurately evaluated with a study of a larger population.

Conclusion

IRIS can significantly reduce image noise and improve the imaging of coronary artery calcifications and stents. The sharp kernel images constructed with IRIS can increase the image quality of coronary CT angiography for the evaluation of coronary calcifications and stents.

Conflict of interest: None declared.

Peer-review: Externally peer-reviewed.

Authorship contributions: Concept - T.H.; Design - D.A., M.K., T.H.; Supervision - D.A., M.K., T.H.; Resource - D.A., M.K., T.H.; Data collection &/or processing - E.G., V.V., E.Ü., I.Ç.K.; Analysis &/or interpretation - E.G., V.V., E.Ü., I.Ç.K., T.H.; Literature search - E.G., V.V., E.Ü., I.Ç.K.; Writing - E.G., T.H.; Critical review - D.A., M.K., T.H.

References

1. Leschka S, Alkadhi H, Plass A, Desbiolles L, Grünenfelder J, Marincek B, et al. Accuracy of MSCT coronary angiography with 64 slice technology: first experience. Eur Heart J 2005; 26: 1482-7. **[CrossRef]**
2. Mollet NR, Cademartiri F, van Mieghem CA, Runza G, McFadden EP, Baks T, et al. High- resolution spiral computed tomography coronary angiography in patients referred for diagnostic conventional coronary angiography. Circulation 2005; 112: 2318-23. **[CrossRef]**
3. Leber AW, Johnson T, Becker A, von Ziegler F, Tittus J, Nikolaou K, et al. Diagnostic accuracy of dual-source multi-slice CT-coronary angiography in patients with an intermediate pretest likelihood for coronary artery disease. Eur Heart J 2007; 28: 2354-60. **[CrossRef]**
4. Sabarudin A, Sun Z, Ng KH. A systematic review of radiation dose associated with different generations of multidetector CT coronary angiography. J Med Imaging Radiat Oncol 2012; 56: 5-17. **[CrossRef]**
5. Kalender WA, Wolf H, Suess C, Gies M, Greess H, Bautz WA. Dose reduction in CT by on-line tube current control: principles and validation on phantoms and cadavers. Eur Radiol 1999; 9: 323-8. **[CrossRef]**
6. Hausleiter J, Martinoff S, Hadamitzky M, Martuscelli E, Pschierer I, Feuchtner GM, et al. Image quality and radiation exposure with a low tube voltage protocol for coronary CT angiography results of the PROTECTION II Trial. JACC Cardiovasc Imag 2010; 3: 1113-23. **[CrossRef]**
7. Stolzmann P, Leschka S, Scheffel H, Krauss T, Desbiolles L, Plass A, et al. Dual-source CT in step-and-shoot mode: noninvasive coronary angiography with low radiation dose. Radiology 2008; 249: 71-80. **[CrossRef]**
8. Park EA, Lee W, Kim KW, Kim KG, Thomas A, Chung JW, et al. Iterative reconstruction of dual-source coronary CT angiography: assessment of image quality and radiation dose. Int J Cardiovasc Imaging 2012; 28: 1775-86. **[CrossRef]**
9. Leipsic J, Heilbron BG, Hague C. Iterative reconstruction for coronary CT angiography: finding its way. Int J Cardiovasc Imaging 2012; 28: 613-20. **[CrossRef]**
10. Sheth T, Dodd JD, Hoffmann U, Abbara S, Finn A, Gold HK, et al. Coronary stent assessability by 64 slice multi-detector computed tomography. Catheter Cardiovasc Interv 2007; 69: 933-8. **[CrossRef]**
11. Hamon M, Biondi-Zoccai GG, Malagutti P, Agostoni P, Morello R, Valgimigli M, et al. Diagnostic performance of multislice spiral

computed tomography of coronary arteries as compared with conventional invasive coronary angiography: a meta-analysis. J Am Coll Cardiol 2006; 48: 1896-910. **[CrossRef]**

12. Stein PD, Beemath A, Kayalı F, Skaf E, Sanchez J, Olson RE. Multidetector computed tomography for the diagnosis of coronary artery disease: a systematic review. Am J Med 2006; 119: 203-16. **[CrossRef]**

13. Renker M, Nance JW Jr, Schoepf UJ, O'Brien TX, Zwerner PL, Meyer M, et al. Evaluation of heavily calcified vessels with coronary CT angiography: comparison of iterative and filtered back projection image reconstruction. Radiology 2011; 260: 390-9. **[CrossRef]**

14. Oda S, Utsunomiya D, Funama Y, Takaoka H, Katahira K, Honda K, et al. Improved coronary in-stent visualization using a combined high-resolution kernel and a hybrid iterative reconstruction technique at 256-slice cardiac CT-Pilot study. Eur J Radiol 2013; 82: 288-95. **[CrossRef]**

15. Mahnken AH. CT imaging of coronary stents: past, present and future. ISRN Cardiol 2012; 2012: 139823.

16. Ebersberger U, Tricarico F, Schoepf UJ, Blanke P, Spears JR, Rowe GW, et al. CT evaluation of coronary artery stents with iterative image reconstruction: improvements in image quality and potential for radiation dose reduction. Eur Radiol 2013; 23: 125-32. **[CrossRef]**

17. Hou Y, Liu X, Xv S, Guo W, Guo Q. Comparisons of ımage quality and radiation dose between iterative reconstruction and filtered back projection reconstruction algorithms in 256-MDCT coronary angiography. AJR Am J Roentgenol 2012; 199: 588-94. **[CrossRef]**

18. Wang R, Schoepf UJ, Wu R, Gibbs KP, Yu W, Li M, et al. CT coronary angiography: Image quality with sinogram affirmed iterative reconstruction compared with filtered back-projection. Clin Radiol 2013; 68: 272-8. **[CrossRef]**

19. Hou Y, Xu S, Guo W, Vembar M, Guo Q. The optimal dose reduction level using iterative reconstruction with prospective ECG-triggered coronary CTA using 256-slice MDCT. Eur J Radiol 2012; 81: 3905-11. **[CrossRef]**

20. Bittencourt MS, Schmidt B, Seltmann M, Muschiol G, Ropers D, Daniel WG, et al. Iterative reconstruction in image space (IRIS) in cardiac computed tomography: initial experience. Int J Cardiovasc Imaging 2011; 27: 1081-7. **[CrossRef]**

21. Zhou Q, Jiang B, Dong F, Huang P, Liu H, Zhang M. Computed tomography coronary stent imaging with iterative reconstruction: a trade-off study between medium kernel and sharp kernel. J Comput Assist Tomogr 2014; 38: 604-12. **[CrossRef]**